

Prioritized Subnet Sampling for Resource-Adaptive Supernet Training

Bohong Chen¹, Mingbao Lin¹, Liujuan Cao¹, Jianzhuang Liu², Qixiang Ye³,
Baochang Zhang⁴, Wei Zeng⁵, Yonghong Tian⁵, Rongrong Ji^{1,6*}

¹School of Informatics, Xiamen University

²Noah’s Ark Lab, Huawei Technologies

³University of Chinese Academy of Sciences

⁴Beihang University ⁵Peking University

⁶Institute of Artificial Intelligence, Xiamen University

Abstract

A resource-adaptive supernet adjusts its subnets for inference to fit the dynamically available resources. In this paper, we propose Prioritized Subnet Sampling to train a resource-adaptive supernet, termed PSS-Net. We maintain multiple subnet pools, each of which stores the information of substantial subnets with similar resource consumption. Considering a resource constraint, subnets conditioned on this resource constraint are sampled from a pre-defined subnet structure space and high-quality ones will be inserted into the corresponding subnet pool. Then, the sampling will gradually be prone to sampling subnets from the subnet pools. Moreover, the one with a better performance metric is assigned with higher priority to train our PSS-Net, if sampling is from a subnet pool. At the end of training, our PSS-Net retains the best subnet in each pool to entitle a fast switch of high-quality subnets for inference when the available resources vary. Experiments on ImageNet using MobileNetV1/V2 show that our PSS-Net can well outperform state-of-the-art resource-adaptive supernets. Our project is at <https://github.com/chenbong/PSS-Net>.

Introduction

Deep neural networks (DNNs) have advanced many tasks of artificial intelligence. Traditional DNNs are designed with a fixed network structure, where the hardware resources, such as computation ability and memory footprint, have to be allocated in advance to enable the running of DNNs. Unfortunately, the equipped resources are greatly different among heterogeneous devices. Even for the same device, the availability of hardware resources varies over time. These limitations considerably barricade DNNs to be deployed. Though many works obtain a compact network via model compression (Ruan et al. 2021; Wang et al. 2020; Liu et al. 2019), network architecture search (NAS) (Cai et al. 2020; Dai et al. 2019), *etc.*, the resulting model structures are still fixed, making it hard to make full use of hardware resources.

By adjusting the runtime subnets to fit the dynamically available resources, designing resource-adaptive supernets has attracted increasing attention from the research community. According to the subnet sampling strategy during supernet training, traditional resource-adaptive supernets can be generally divided into two groups including uniform subnet sampling and random subnet sampling.

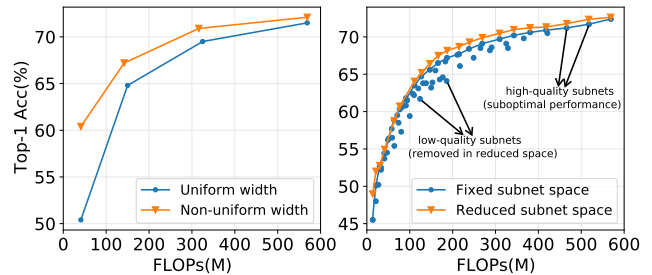


Figure 1: **Left:** Performance of SlimmableNetwork (Yu et al. 2019) with uniform width and non-uniform width (Liu et al. 2019). **Right:** Performance of MutualNet (Yang et al. 2020) with fixed and reduced search spaces.

For uniform subnet sampling, some fixed multipliers are applied to all layers to scale the network width, thus enabling to switch subnets with different uniform widths at runtime (Yu et al. 2019; Yu and Huang 2019b). In addition to uniform width, (Yang et al. 2020) further considered the resolution of input images to enhance subnet performance. As for random subnet sampling, these methods (Cai et al. 2020; Lou et al. 2021; Yu et al. 2020; Wang et al. 2021) randomly sample subnets from a supernet for training in each iteration, and then search for optimal subnets of different sizes from the pre-trained supernet using heuristics algorithms. The learning is also known as one-shot NAS. Nevertheless, the performance is still far from satisfactory for real-world applications. We attribute it to three open issues, *i.e.*, *homogeneity of subnets*, *search overhead*, and *subnet mismatch*.

In terms of homogeneity of subnets, uniform subnet sampling (Yu et al. 2019; Yu and Huang 2019b; Yang et al. 2020) simply enforces shared multipliers to all layers without investigating the diversity of layer-wise width. Consequently, only one subnet structure can be made given a particular resource constraint such as FLOPs, latency, *etc.* As previously studied in network pruning (Yu and Huang 2019a; Lin et al. 2020b; Liu et al. 2019) and NAS (Guo et al. 2020b; Cai et al. 2020), the optimal subnet at a particular size often results from the non-uniform sampling. To verify this, we perform a validation experiment on ImageNet by replacing the uniform width of MobileNetV1 (Yu et al. 2019) with a non-uniform form from (Liu et al. 2019). Fig. 1(Left) shows a better trade-off between accuracy and FLOPs from the non-

*Corresponding Author: rrji@xmu.edu.cn

uniform strategy. Thus, the homogeneity of subnets, if not well addressed, often results in suboptimal performance.

In terms of search overhead, though random subnet sampling may produce different subnet structures over supernet training with respect to a particular resource, which partially alleviates the homogeneity of subnets, additional overheads are required to search for the optimal subnet of a particular size for inference. As reported by (Cai et al. 2020), it takes around 40 GPU hours to find out each target subnet in the trained supernet. Though this additional cost is acceptable in offline environment, it greatly prevents resource-adaptive supernet from real-time running environment where the available hardware resources frequently vary a lot due to the concurrently running applications.

Subnet mismatch refers to that the sampled subnets during training deviate considerably from the target subnets in inference (Yang et al. 2020; Cai et al. 2020; Lou et al. 2021). For example, (Yang et al. 2020) observed that only around 30% of sampled subnets fall into the trade-off curve of accuracy *v.s.* FLOPs. This indicates that a large amount of computation is wasted on training these low-quality subnets that would not be considered in inference. Besides, without sufficient training, these high-quality subnets may result in suboptimal performance in the real-world applications as shown in Fig. 1(Right). Thus, it is necessary to gradually reduce the subnet structure space during the network training, so as to concentrate more on these high-quality subnets, which is also discussed by (Sahni et al. 2021).

Overall, challenges still remain in training a resource-adaptive supernet. On one hand, we pursue high-performing DNNs for practical deployment. On the other hand, the deployed model should be switchable instantly if the available hardware resources are changed. Reflecting upon the subnet mismatch problem mentioned above, we can know that uniform subnet sampling and random subnet sampling fail to accurately model subnets towards the available resources. Therefore, a tedious search process has to be executed to find out the target subnet each time the available resources vary.

To solve the aforementioned problems, in this paper, we propose prioritized subnet sampling to train a resource-adaptive supernet, termed PSS-Net, as illustrated in Fig. 2. We first build a subnet structure space by applying varying multipliers to different layers, which eliminates the homogeneity of subnets resulting from uniform subnet sampling. Then, we set up a group of subnet pools, each of which stores the information of these high-quality subnets conditioned on the same resource constraint. In the early training batches of our PSS-Net, we sample a medium-sized subnet from a pre-built subnet structure space according to the structure distribution (Wang et al. 2021). To measure the quality of a sampled subnet, we consider its batch loss as the performance metric, alternative to validation accuracy which requires a computationally heavy subnet training. We update the performance metric using moving average if the same subnet structure is sampled multiple times. For each high-quality subnet, its information is inserted into the corresponding subnet pool. When the subnet pool is full, subnet sampling will gradually shift from the subnet structure space to each subnet pool to ensure that high-quality subnets are

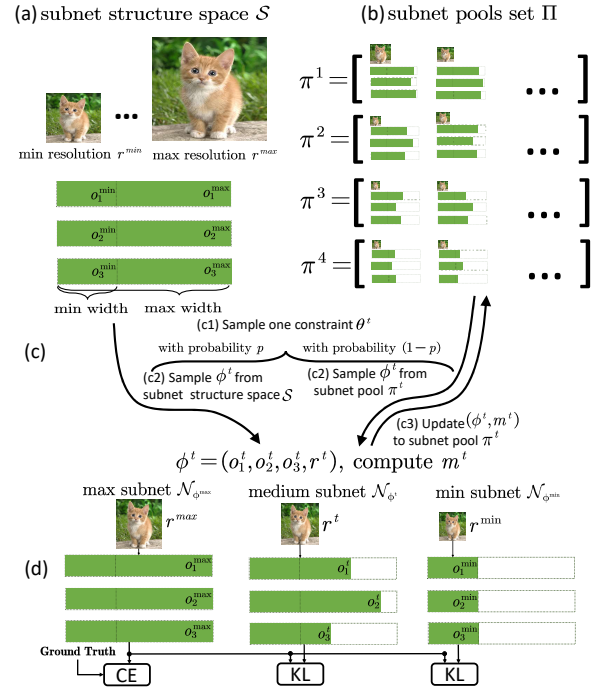


Figure 2: PSS-Net training framework. (a) Initializing the subnet structure space \mathcal{S} . (b) Setting up a set of subnet pools $\Theta = \{\pi^1, \pi^2, \dots, \pi^T\}$. (c) Given a resource constraint θ^t , sampling a medium-sized subnet structure ϕ^t either from the subnet structure space \mathcal{S} , or from the corresponding subnet pool π^t . (d) Slimmable training for $\mathcal{N}_{\phi^{max}}, \mathcal{N}_{\phi^t}, \mathcal{N}_{\phi^{min}}$.

entitled with sufficient training, which solves the problem of subnet mismatch. Moreover, when sampling is from a subnet pool, the one with a better performance metric than other high-quality subnets is given with higher priority to be sampled to train PSS-Net. At the end of PSS-Net training, we only need to preserve the best subnet in each pool. Consequently, PSS-Net results in a set of subnets that can be alternatively deployed to adapt to the currently available resources, without additional overhead for subnet search.

We use the challenging MobileNetV1 (Howard et al. 2017) and MobileNetV2 (Sandler et al. 2018) as our supernets, and the experiments are conducted on ImageNet. The results show that our PSS-Net significantly outperforms the state-of-the-arts under different resource constraints including FLOPs, CPU latency and GPU latency.

Related Work

We briefly discuss the major topics that are most related to resource-adaptive supernets.

Compact Networks. To overcome the hurdle of deploying models on resource-limited devices, many previous works focus on obtaining compact networks, typically through model compression (Guo, Ouyang, and Xu 2020a; Ruan et al. 2021; Wang et al. 2020; Li et al. 2020; Liu et al. 2019), network architecture search (NAS) (Wang et al. 2021; Cai et al. 2020; He et al. 2018), *etc.* Network pruning, a form of model compression, removes redundant weights/filters to satisfy resource constraints in general hardware. (Han

et al. 2015) proposed to recursively remove small-magnitude weights and retrain the ℓ_2 -regularized subnetwork to recover accuracy. (Lin et al. 2020a) discarded filters with low-rank feature map outputs. The lottery ticket hypothesis (Frankle and Carbin 2018) randomly initializes a dense network and trains it from scratch. The subnets with high-weight values are extracted, and retrained with the initial weight values of the original dense model. (Guo, Ouyang, and Xu 2020b) also considered multi-dimension pruning including output channels, model depth, input resolution, *etc.* Different from model compression operating upon an existing backbone network, NAS (Zoph and Le 2017; Wang et al. 2021; Cai et al. 2020; Yu et al. 2020) conducts search on a space of network structures including operations, width, depth, *etc.*, to obtain a compact model. The broader search space brings about better performance as reported in existing studies.

Sample-Adaptive Networks. A sample-adaptive network adapts its structure according to the input image samples. (Lin et al. 2017) modeled the adaption of network width as a Markov decision process, and measured the convolutional kernel importance conditioned on different samples. (Bejnordi, Blankevoort, and Welling 2020) adjusted the network width via a gating module conditioned on the current input. To this end, a ‘‘batch-shaping’’ is introduced to match the marginal aggregated posterior distribution over any intermediate features to a pre-specified prior distribution. Except for adjusting network width, another group realizes sample-adaptive network from the perspective of depth adaption. For instance, (Huang et al. 2018) proposed to early exist from the inference at shallow layers of the network through training multiple classifiers upon intermediate features. SkipNet (Wang et al. 2018) skips convolutional blocks via a gating network that maps the last-layer outputs to a binary decision to execute or bypass the current layer.

Traditional compact networks are fixed for deployment. A sample-adaptive network allocates more computational resources to complex images, and fewer to images that are easier for the task. As a core distinction, our PSS-Net produces multiple subnets and switches these subnets for deployment according to available hardware resources.

Methodology

Preliminary

Our PSS-Net is an L -layers supernet $\mathcal{N}_{\phi^{max}, \mathbf{W}}$ with structure $\phi^{max} = (\{o_i^{max}\}_{i=1}^L, r^{max})$ and weights $\mathbf{W} = \{\mathbf{W}_i\}_{i=1}^L$, where o_i^{max} , r^{max} and \mathbf{W}_i are the number of output channels in the i -th layer, the supernet input resolution, and the weights of the i -th layer, respectively. The supernet $\mathcal{N}_{\phi^{max}, \mathbf{W}}$ contains subnets of multiple sizes, and each subnet $\mathcal{N}_{\phi^t, \mathbf{W}^t}$ is allowed to use a different subnet structure $\phi^t = (\{o_i^t\}_{i=1}^L, r^t)$ and subnet weights $\mathbf{W}^t = \{\mathbf{W}_i[1 : o_i^t]\}_{i=1}^L$, similarly, where o_i^t and r^t are the number of output channels in the i -th layer and the subnet input resolution, respectively. $\mathbf{W}_i[1 : o_i^t]$ means the subnet weights of the i -th layer are the weights of the first o_i^t channels in \mathbf{W}_i . Therefore, any two subnets share partial weights. Then we set separate lower bounds for each layer of the subnet structure $\{o_i^t\}_{i=1}^L$ and r^t as $\{o_i^{min}\}_{i=1}^L$ and r^{min} , *i.e.*,

the structure of the smallest subnet can be represented as $\phi^{min} = (\{o_i^{min}\}_{i=1}^L, r^{min})$. Finally, we can represent the subnet structure space as $\mathcal{S} = \{\phi^1 = (\{o_i^1\}_{i=1}^L, r^1), \phi^2 = (\{o_i^2\}_{i=1}^L, r^2), \dots\}$, where $o_i^{min} \leq o_i^t \leq o_i^{max}$, $r^{min} \leq r^t \leq r^{max}$. In practice, for any subnet $\mathcal{N}_{\phi^t, \mathbf{W}^t}$, where the structure $\phi^t = (\{o_i^t\}_{i=1}^L, r^t) \in \mathcal{S}$, we sample o_i^t from $\{o_i^{min}, o_i^{min} + 1, o_i^{min} + 2, \dots, o_i^{max}\}$ and then round to its nearest multiple of 8 to obtain a hardware friendly channel number, and r^t is sample from $\{r^{min}, r^{min} + 8, r^{min} + 16, \dots, r^{max}\}$.

Given a set of resource constraints $\Theta = \{\theta^t\}_{t=1}^T$, our goal is to train $\mathcal{N}_{\phi^{max}, \mathbf{W}}$ such that T subnets $\{\mathcal{N}_{\phi^t, \mathbf{W}^t} | \phi^t \in \mathcal{S}, \mathbf{W}^t \in \mathbf{W}\}_{t=1}^T$ conditioned on Θ can be obtained from this supernet. We define this problem as:

$$\begin{aligned} & \{(\phi^t)_{best}\}_{t=1}^T, \{(\mathbf{W}^t)_{best}\}_{t=1}^T \\ &= \arg \max_{\{\phi^t\}_{t=1}^T, \{\mathbf{W}^t\}_{t=1}^T} \sum_{t=1}^T Acc(\mathcal{N}_{\phi^t, \mathbf{W}^t}), \quad (1) \\ & \text{s.t. } \phi^t \in \mathcal{S}, \theta^t \in \Theta, \mathcal{C}(\mathcal{N}_{\phi^t, \mathbf{W}^t}) \in [\theta^t - \delta, \theta^t + \delta], \end{aligned}$$

where $\mathcal{C}(\mathcal{N}_{\phi^t, \mathbf{W}^t})$ is a function to calculate the resource consumption of subnet $\mathcal{N}_{\phi^t, \mathbf{W}^t}$, δ is a bias tolerance between actual resource consumption and the given resource constraint θ^t , and $Acc(\mathcal{N}_{\phi^t, \mathbf{W}^t})$ returns the accuracy of $\mathcal{N}_{\phi^t, \mathbf{W}^t}$ on the validation set. Note that, each subnet weights are a subset of the supernet weights, *i.e.*, $\mathbf{W}^t \in \mathbf{W}$. Thus, to update \mathbf{W}^t is to update \mathbf{W} in essence. For simplicity, we remove the superscript ‘‘ t ’’ in \mathbf{W}^t and Eq. (1) can be simplified as:

$$\begin{aligned} & \{(\phi^t)_{best}\}_{t=1}^T, (\mathbf{W})_{best} = \arg \max_{\{\phi^t\}_{t=1}^T, \mathbf{W}} \sum_{t=1}^T Acc(\mathcal{N}_{\phi^t, \mathbf{W}}), \\ & \text{s.t. } \phi^t \in \mathcal{S}, \theta^t \in \Theta, \mathcal{C}(\mathcal{N}_{\phi^t, \mathbf{W}}) \in [\theta^t - \delta, \theta^t + \delta]. \quad (2) \end{aligned}$$

To train each subnet $\mathcal{N}_{\phi^t, \mathbf{W}}$ in Eq. (1), (Yu and Huang 2019b) proposed a three-step slimmable training paradigm: The ‘‘sandwich rule’’ is firstly adopted to select three subnet types of one maximal size (*i.e.*, the supernet, $\mathcal{N}_{\phi^{max}, \mathbf{W}}$), several medium sizes and one minimal size (*i.e.*, the minimal subnet $\mathcal{N}_{\phi^{min}, \mathbf{W}}$). Then, the inplace distillation is conducted between the supernet and other subnets. Finally, the parameters in the batch normalization layers of the subnets are recalibrated after training. This paradigm has inspired many subsequent researches to train resource-adaptive supernets or compact networks (Yang et al. 2020; Cai et al. 2020; Lou et al. 2021; Yu et al. 2020; Wang et al. 2021). The main difference between these approaches lies in the selection of the medium-sized subnets in the ‘‘sandwich rule’’ step. Traditional approaches (Yu and Huang 2019b; Yang et al. 2020) obtain a medium-sized subnet using uniform subnet sampling, *i.e.*, applying a fixed width multiplier to all layers in each batch training. However, such a manner causes suboptimal performance due to the homogeneity of subnets. The one-shot NAS (Lou et al. 2021; Yu et al. 2020; Wang et al. 2021) randomly samples medium-sized subnets from the pre-defined subnet structure space \mathcal{S} to train the supernet. However, heavy cost is inevitable to search for the target subnet each time the available hardware resources change.

Algorithm 1: PSS-Net Training

Input: Supernet weight \mathbf{W} , supernet structure ϕ^{max} , minimal subnet structure ϕ^{min} , resource constraints $\Theta = \{\theta^t\}_{t=1}^T$, subnet structure space \mathcal{S} .

Output: best subnet structures $\{(\phi^t)_{best}\}_{t=1}^T$, Trained supernet weights $(\mathbf{W})_{best}$.

```
1: Initialize subnet pools set:  $\Pi = \{\pi^t = \{\}\}_{t=1}^T$ .  
   #  $e$ : training epoch number,  $b$ : training batch number.  
2: for  $e = 1, \dots, E$  do  
3:   for  $b = 1, \dots, B$  do  
4:      $subnet\_list = \{\phi^{max}\}$ ;  
5:     Randomly sample  $t$  from  $\{1, 2, \dots, T\}$ ;  
6:      $\phi^t, \pi^t = \text{Alg. 2}(\theta^t, \pi^t, \mathcal{S}, e, E)$ ;  
7:      $subnet\_list = subnet\_list \cup \{\phi^t, \phi^{min}\}$ ;  
8:      $\mathbf{W} = \text{slimmable\_training}(\mathbf{W}, subnet\_list)$ ;  
   # Details of slimmable\_training can be found in the appendix.  
9:   end for  
10: end for  
11: for  $t$  in  $1, \dots, T$  do  
12:   for  $j$  in  $1, \dots, M$  do  
13:     Calibrate BN statistics of subnet  $\mathcal{N}_{\phi_j^t, \mathbf{W}}$ ;  
14:     Compute  $\text{Acc}(\mathcal{N}_{\phi_j^t, \mathbf{W}})$  on the validation set;  
15:   end for  
16:    $(\phi^t)_{best}, (\mathbf{W})_{best} = \arg \max_{(\phi^t)_j, \mathbf{W}} \text{Acc}(\mathcal{N}_{(\phi^t)_j, \mathbf{W}})$ .  
17: end for  
18: return  $\{(\phi^t)_{best}\}_{t=1}^T, (\mathbf{W})_{best}$ .
```

PSS-Net Training

To solve the above problems, we propose prioritized subnet sampling to sample the medium-sized subnet for training our supernet, termed PSS-Net in this paper. Our PSS-Net training generally follows the three-step slimmable training paradigm as shown in Fig. 2. We first outline our PSS-Net training in Alg. 1, which is then detailed below.

Subnet Pools (Line 1, Alg. 1). Different from traditional slimmable training paradigm, our PSS-Net training maintains a set of subnet pools, denoted as $\Pi = \{\pi^t = \{\}\}_{t=1}^T$. The t -th subnet pool π^t is used to collect the information of M high-quality subnets conditioned on the resource constraint θ^t in Eq. (2). The information of each subnet includes its network structure ϕ^t and performance metric m^t , which will be detailed in the next section.

Slimmable Training (Line 2 – Line 10, Alg. 1). In each training batch, we select three subnet types of one maximal size (*i.e.*, the supernet, $\mathcal{N}_{\phi^{max}, \mathbf{W}}$), one medium size and one minimal size (*i.e.*, the minimal subnet $\mathcal{N}_{\phi^{min}, \mathbf{W}}$). The “slimmable_training” in Line 8 of Alg. 1 is the same as Line 3 – Line 16 of Alg. 1 in USNet (Yu and Huang 2019b) and is elaborated in the appendix. To obtain a medium-sized subnet ϕ^t , USNet applies a fixed width multiplier to uniformly reduce the width of the supernet, whereas with the aid of the introduced subnet pools, our PSS-Net gives priority to high-quality subnets, as outlined in Alg. 2 and detailed in the next section.

Algorithm 2: Prioritized Subnet Sampling

Input: Subnet pool π^t conditioned on resource constraint θ^t , subnet structure space \mathcal{S} , current epoch e , and total epochs E .

Output: Subnet structure ϕ^t , and subnet pool π^t

```
1:  $p = p_{end}^{\mathcal{I}(|\pi^t| < M) \cdot (e-1)/E}$ ;  
2: if  $\text{rand}(0, 1) < p$  then  
3:   Sample a subnet structure  $\phi^t \in \mathcal{S}$ , s.t.  $\mathcal{C}(\mathcal{N}_{\phi^t, \mathbf{W}}) \in [\theta^t - \delta, \theta^t + \delta]$  using Eq. (4);  
4: else  
5:    $\eta = \eta_{end}^{\mathcal{I}(|\pi^t| < M) \cdot (e-1)/E}$ ;  
6:   Sample a subnet structure  $\phi^t \in \pi^t$  using Eq. (6);  
7: end if  
8: if  $\phi^t$  not in  $\pi^t$  then  
9:    $m^t = -batch\_loss$ ;  
10:  Insert  $(\phi^t, m^t)$  into  $\pi^t$ ;  
11:  if  $|\pi^t| > M$  then  
12:    Remove  $((\phi^t)_M, (m^t)_M)$ ;  
13:  end if  
14: else  
15:    $m^t = \lambda \cdot m^t + (1 - \lambda) \cdot (-batch\_loss)$ ;  
16:   Update  $m^t$  of  $\phi^t$  in  $\pi^t$ .  
17: end if  
18: return  $\phi^t, \pi^t$ .
```

BN Calibration (Line 11 – Line 17, Alg. 1). After the slimmable training, each subnet pool $\pi^t \in \Pi$ will be filled with these high-quality subnets conditioned on its corresponding resource constraint θ^t . However, the statistics in the batch normalization (BN) layers of these high-quality subnets are not accurately estimated since the forward propagated subnets vary during training our PSS-Net. As a consequence, BN calibration is indispensable in order to evaluate the performance of each subnet. To this end, following (Yu and Huang 2019b; Yang et al. 2020), we feed each subnet with a small training set of 8, 192 images in this paper to update the BN statistics of each subnet in π^t . Then, the calibrated subnet with the best accuracy is regarded as the optimal subnet $\mathcal{N}_{(\phi^t)_{best}, (\mathbf{W})_{best}}$ under the resource constraint of θ^t . At the end of training, the subnet pool has collected a sufficient number of high-quality subnet structures for each resource constraint and the corresponding performance metrics detailed in the next section. Thus, we only need to calibrate k subnets within top- k performance metrics, and then pick the one with the best accuracy.

Prioritized Subnet Sampling

We outline our prioritized subnet sampling in Alg. 2, which serves as a core distinction of our work from the previous studies. More details are given below.

Subnet Sampling (Line 1 – Line 7, Alg. 2). As mentioned above, we intend to sample a medium-sized subnet ϕ^t to train our PSS-Net in each training batch. Instead of simply sampling subnets from the subnet structure space \mathcal{S} , we also conduct subnet sampling from the subnet pool π^t given the resource constraint θ^t . To this end, we introduce a factor

$p \in (0, 1)$ to indicate the probability of sampling from the subnet structure space \mathcal{S} . At the beginning of PSS-Net training, we sample subnets from \mathcal{S} until π^t is full. In this situation, we expect $p = 1$. As the training of PSS-Net, more high-quality structures of subnets will be inserted into π^t , and we expect to give priority to sampling from π^t , which indicates a small value of p . To this end, we formalize p as:

$$p = p_{end}^{\mathcal{I}(|\pi^t| < M) \cdot (e-1)/E}, \quad (3)$$

where p_{end} is a pre-given parameter indicating the probability of sampling from the subnet structure space \mathcal{S} when PSS-Net training ends. In our implementation, we set $p_{end} = 0.01$. $\mathcal{I}(\cdot)$ is an indicator which returns 1 if the input is true, and 0 otherwise. The $e \in [1, E]$ and E respectively denote the current training epoch and the total training epochs. As can be seen, starting from 1, the probability of sampling from \mathcal{S} decreases to p_{end} gradually. Consequently, the priority will be entitled to the high-quality subnets.

Case 1: Sampling from the subnet structure space \mathcal{S} (Line 3 – Line 4, Alg. 2). To sample a subnet $\mathcal{N}_{\phi^t, \mathbf{w}}$ conditioned on θ^t , one naive solution is to go through trial and error until an eligible subnet is found. However, this strategy brings heavy cost. Usually, thousands of sampling are inevitable each time according to our experimental observation. Inspired by (Wang et al. 2021), we resort to the probability distribution of subnets conditioned on the given resource constraint θ^t , denoted as $\tau(\phi = \{o_i\}_{i=1}^L | \theta^t)$. However, the practical distribution is extremely complex to describe. While the Monte-Carlo approximation can be adopted, it is still intractable since multiple approximations have to be repeatedly constructed for each resource constraint $\theta^t \in \Theta$. To overcome this, we first generate a large-scale set of subnet structures \mathcal{G} , and then compute the practical resource consumption of each structure $\phi \in \mathcal{G}$ as $\mathcal{C}(\mathcal{N}_{\phi, \mathbf{w}})$. Finally, we split \mathcal{G} into T non-overlapping subsets with $\mathcal{G}^1 \cup \mathcal{G}^2 \cup \dots \cup \mathcal{G}^T = \mathcal{G}$. For each subnet structure $\phi^t \in \mathcal{G}^t$, its resource consumption satisfies that $\mathcal{C}(\mathcal{N}_{\phi^t, \mathbf{w}}) \in [\theta^t - \sigma, \theta^t + \sigma]$. To model $\tau(\phi^t = \{o_i^t\}_{i=1}^L | \theta^t)$, we directly estimate the marginal probability of $\tau(o_i^t | \theta^t)$ as:

$$\tau(o_i^t | \theta^t) \approx \frac{\sum_{\phi^t = \{o_k^t\}_{k=1}^L \in \mathcal{G}^t} \mathcal{I}(o_k^t = o_i^t)}{|\mathcal{G}^t|}. \quad (4)$$

With Eq. (4), the sampling times to find the target subnet reduces from 10^6 to 10^1 approximately according to our observation, which greatly improves the sampling efficiency.

Case 2: Sampling from the subnet pool π^t (Line 5 – Line 7, Alg. 2). For $\pi^t = \{((\phi^t)_j, (m^t)_j)\}_{j=1}^M$, to obtain the best subnet conditioned on θ^t in Eq. (2), we resort to preserving the best subnet structure in π^t for deployment, *i.e.*,

$$(\phi^t)_{best} = \arg \max_{(\phi^t)_j} \text{Acc}(\mathcal{N}_{(\phi^t)_j, \mathbf{w}}), \quad (5)$$

after our PSS-Net training. Thus, it is natural to prioritize the subnet structure with the best performance m^t in π^t to train our PSS-Net. To this end, we perform weighted sampling upon π^t so that better subnets are assigned with higher probabilities. Thus, we can obtain a distribution set $\{(q^t)_j\}_{j=1}^M$

with $\sum_{j=1}^M (q^t)_j = 1$ where $(q^t)_j$ denotes the probability of sampling $(\phi^t)_j$ to train PSS-Net, which is defined as:

$$(q^t)_j = \frac{\exp((m^t)_j / \eta)}{\sum_{i=1}^M \exp((m^t)_i / \eta)}, \quad (6)$$

where η is a temperature to control the smoothness of the distribution. In the early training stage, the subnets are not well trained, and thus m^t is not a reliable measure to reflect the actual performance of each subnet. At this time, we expect each subnet to be sampled equally. As training goes, m^t will become stable and we expect the distribution to be a one-hot form. Similar to Eq. (3), we achieve this by setting $\eta = \eta_{end}^{\mathcal{I}(|\pi^t| < M) \cdot (e-1)/E}$, where $\eta_{end} = 0.01$.

Subnet Pool Manipulation (Line 8 – Line 16, Alg. 2).

We continuously collect the information tuple (ϕ^t, m^t) until the pool π^t is full. When receiving a (ϕ^t, m^t) , we insert it into π^t such that the information tuples in π^t are arranged in a decreasing order according to the performance m^t . In the case of full pool, we can obtain $\pi^t = \{((\phi^t)_j, (m^t)_j)\}_{j=1}^M$ with $(m^t)_{j+1} \leq (m^t)_j$ and $(\phi^t)_j = \{(o_i^t)_j\}_{i=1}^L$. If one more tuple received, we will remove the worst performing tuple, *i.e.*, $((\phi^t)_M, (m^t)_M)$, before inserting this tuple.

To model m^t of ϕ^t , the best way is to define it as the accuracy of the subnet $\mathcal{N}_{\phi^t, \mathbf{w}}$. However, due to the large subnet structure space, it is almost impossible to execute a complete training for every subnet. Inspired by (Wang et al. 2021; Berman et al. 2020), we define $(m^t)_j = -batch_loss$ if ϕ^t is inserted into π^t for the first time. If ϕ^t is sampled from π^t for updating PSS-Net, we update m^t using moving average as $m^t = \lambda \cdot m^t + (1 - \lambda) \cdot (-batch_loss)$ after the current training batch. Here, we define $batch_loss$ as the training loss in the current batch.

Experiments

Experimental Settings

We use the light-weight MobileNetV1 (Howard et al. 2017) and MobileNetV2 (Sandler et al. 2018) as the backbones of PSS-Net and compared methods, and then conduct experiments on ImageNet (Deng et al. 2009). We set o_i^{max} to be the same as the channel number of the i -th layer in the backbone network, and r^{max} is 224. Then we define $o_i^{min} = 0.75 \cdot o_i^{max}$, $r^{min} = 128$. After that we can obtain the supernet $\mathcal{N}_{\phi^{max}, \mathbf{w}}$, and the subnet space \mathcal{S} . We perform three resource constraints in this paper, including FLOPs, CPU latency and GPU latency. The resource constraint set Θ ranges from $\mathcal{C}(\mathcal{N}_{\phi^{min}, \mathbf{w}})$ to $\mathcal{C}(\mathcal{N}_{\phi^{max}, \mathbf{w}})$ with steps of 10M, 10 μ s and 1ms for FLOPs, GPU latency and CPU latency, respectively. The subnet pool size M is set to 50.

We construct lookup tables of CPU and GPU latencies for a quick calculation of resource consumption $\mathcal{C}(\cdot)$ during PSS-Net training. The details of the lookup tables and more ablation studies are provided in the appendix.

Experimental Results

Comparison with Resource-Adaptive Methods. We first compare our proposed PSS-Net with the resource-adaptive

Backbone	MobileNetV1 569M / 70.6%				MobileNetV2 301M / 72.0%			
Method	USNet	MutualNet	PSS-Net _F	PSS-Net _M	USNet	MutualNet	PSS-Net _F	PSS-Net _M
FLOPs(M)	569 / 71.8	569 / 72.4	555 / 74.2	562 / 74.5	301 / 71.5	301 / 72.9	301 / 73.4	295 / 73.4
/ Acc(%)	306 / 69.1	309 / 69.7	306 / 72.3	309 / 72.5	151 / 67.6	154 / 70.1	154 / 70.7	154 / 70.7
	114 / 61.9	111 / 63.5	107 / 67.9	107 / 68.0	88 / 64.2	84 / 65.8	84 / 66.8	83 / 66.7
Model	USNet	MutualNet	PSS-Net _G	PSS-Net _M	USNet	MutualNet	PSS-Net _G	PSS-Net _M
GPU_lat(μ s)	238 / 71.8	238 / 72.4	238 / 74.4	236 / 74.5	269 / 71.5	275 / 72.9	260 / 73.4	260 / 73.4
/ Acc(%)	138 / 66.3	132 / 68.4	128 / 71.9	131 / 71.8	229 / 62.3	207 / 71.0	197 / 72.5	197 / 72.4
	76 / 57.3	80 / 63.5	76 / 68.1	71 / 68.1	/	105 / 64.2	101 / 66.5	102 / 66.7
Model	USNet	MutualNet	PSS-Net _C	PSS-Net _M	USNet	MutualNet	PSS-Net _C	PSS-Net _M
CPU_lat(ms)	36 / 71.8	37 / 72.4	32 / 74.2	30 / 74.5	41 / 71.5	41 / 72.9	30 / 73.2	33 / 73.4
/ Acc(%)	22 / 67.8	21 / 68.4	21 / 72.8	21 / 72.5	/	25 / 71.0	23 / 72.4	26 / 72.4
	13 / 61.0	13 / 63.5	13 / 68.3	13 / 68.6	/	17 / 64.2	17 / 69.0	18 / 68.2

Table 1: Performance comparison with the resource-adaptive methods (Yu and Huang 2019b; Yang et al. 2020).

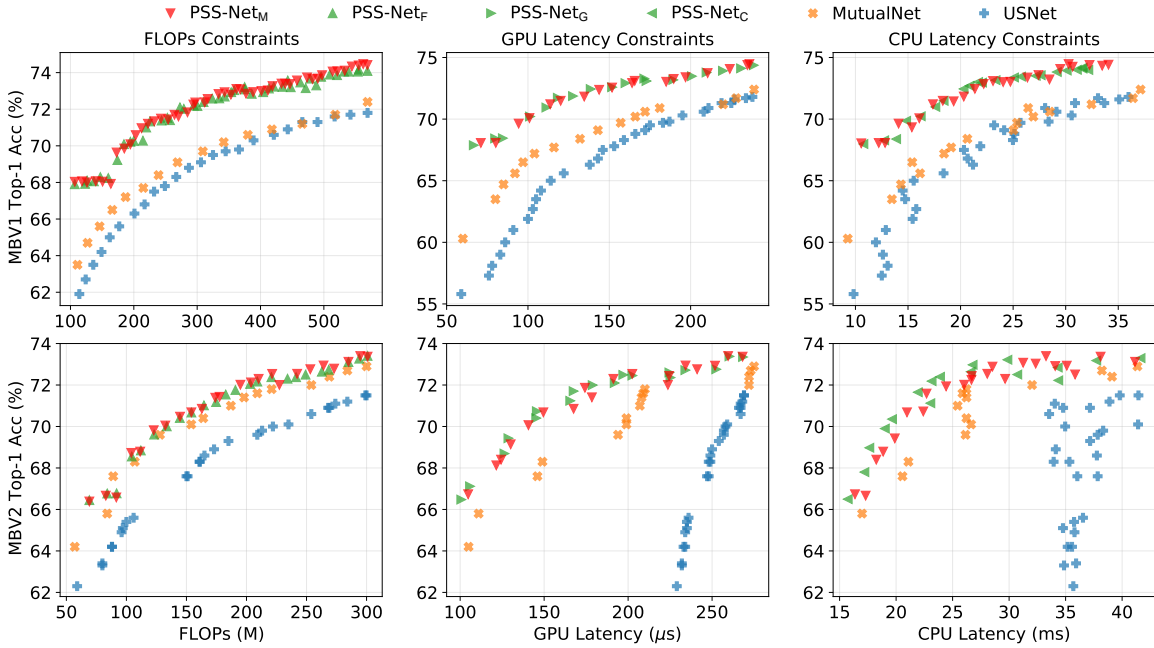


Figure 3: MobileNetV1/V2 experiments under single and multiple types of resource constraints.

studies (Yu and Huang 2019b; Yang et al. 2020). We train four types of PSS-Net constrained by different resources including: (1) PSS-Net_F is trained under only FLOPs constraint; (2) PSS-Net_C is trained under only CPU latency constraint; (3) PSS-Net_G is trained under only GPU latency constraint; (4) PSS-Net_M is trained under multiple constraints of FLOPs, CPU latency and GPU latency.

In Tab. 1, we respectively compare the accuracies of the subnets resulting from different methods under similar FLOPs, GPU latency and CPU latency. Some observations can be found from Tab. 1. First, our PSS-Net provides subnets with better performance when compared to MutualNet (Yang et al. 2020) and USNet (Yu and Huang 2019b) under similar or less resource consumption on FLOPs, GPU latency and CPU latency. Second, USNet using MobileNetV2 as its supernet backbone fails to produce subnets with low GPU/CPU latency. Third, though PSS-Net_M needs to accommodate more resource constraints, its performance is still comparable or even better than PSS-Net_F,

PSS-Net_G and PSS-Net_C dedicated to a single type of resource constraint. Fourth, PSS-Net can significantly improve the performance of the backbone networks, for example, PSS-Net_M increases the accuracy of MobileNetV1/V2 from 70.6%/72.0% to 74.5%/73.4% with reduction on FLOPs.

To better demonstrate the advantage of our PSS-Net over existing studies, we further plot the resource-accuracy curves of different methods in Fig. 3. We can observe that our PSS-Net consistently outperforms USNet and MutualNet by a large margin in all subfigures. Under similar resource consumption, our PSS-Net brings subnets with higher accuracy. In addition, similar to Tab. 1, USNet using MobileNetV2 as the supernet backbone only produces subnets with high GPU/CPU latency. Specifically, the GPU latency is over 225 μ s and the CPU latency is over 30ms. Such a limitation greatly barricades the deployment of USNet, particularly when the available resources are in short supply. The reasons are attributed to two points. First, the input image resolution of USNet is fixed to 224, which is a

Method	FLOPs(M) / Acc(%)	Method	FLOPs(M) / Acc(%)
MobileNetV1	569 / 70.6	MobileNetV2	301 / 72.0
PNAS [★]	588 / 74.2	NASNet [★]	488 / 72.8
DARTS [★]	574 / 73.3	MetaPruning [▼]	291 / 72.7
NASNet [★]	564 / 74.0	PSS-Net_M	295 / 73.4
PFS [▼]	567 / 71.6	PSS-Net_F	294 / 73.3
PSS-Net_F	569 / 74.1	DPFPS [▼]	226 / 71.1
PSS-Net_M	562 / 74.5	MetaPruning [▼]	217 / 71.2
MetaPruning [▼]	324 / 70.9	ChamNet [★]	212 / 71.6
MDP [▼]	309 / 71.2	CC [▼]	215 / 70.9
PSS-Net_F	310 / 72.4	AMC [▼]	211 / 70.8
PSS-Net_M	309 / 72.5	DMCP [▼]	211 / 72.2
PFS [▼]	286 / 70.7	PFS [▼]	210 / 70.9
AMC [▼]	285 / 70.5	MDP [▼]	206 / 71.4
NetAdapt [▼]	284 / 69.1	PSS-Net_M	204 / 72.1
EagleEye [▼]	284 / 70.9	PSS-Net_F	203 / 72.1
MetaPruning [▼]	281 / 70.6	CPLI [▼]	166 / 67.4
PSS-Net_M	278 / 71.8	DMC [▼]	163 / 68.4
PSS-Net_F	273 / 72.1	PSS-Net_F	163 / 70.9
PFS [▼]	150 / 65.5	PSS-Net_M	163 / 70.9
AutoSlim [▼]	150 / 67.9	MetaPruning [▼]	140 / 68.2
MetaPruning [▼]	149 / 66.1	MDP [▼]	139 / 68.8
PSS-Net_F	126 / 68.1	PSS-Net_F	134 / 70.0
PSS-Net_M	118 / 68.1	PSS-Net_M	133 / 70.0

Table 2: Performance comparison with compact models including channel pruning (▼) and NAS (★).

large size and thus results in heavy GPU/CPU latency. Second, USNet adopts uniform subnet sampling, which ignores the diversity of layer-wise width. The resulting subnets are usually hardware-unfriendly. Our PSS-Net searches for the optimal image resolution for each subnet and the sampling strategy is non-uniform, which brings about subnets with low latency. Besides, the prioritized subnet sampling ensures that high-performing subnets are fully trained, which in turn entitles high performance of these low-latency subnets.

Comparison with Compact Models. We compare PSS-Net with some compact models including channel pruning and Network Architecture Search (NAS) methods. Channel pruning methods include PFS (Wang et al. 2020), MetaPruning (Liu et al. 2019), MDP (Liu et al. 2020), AMC (He et al. 2018), NetAdapt (Yang et al. 2018), EagleEye (Li et al. 2020), AutoSlim (Yu and Huang 2019a), DPFPS (Ruan et al. 2021), CC (Li et al. 2021), DMCP (Guo et al. 2020a), CPLI (Guo, Ouyang, and Xu 2020a) and DMC (Gao et al. 2020). NAS methods include DARTS (Liu, Simonyan, and Yang 2019), PNAS (Liu et al. 2018), NASNet (Zoph et al. 2018) and ChamNet (Dai et al. 2019). We compare the accuracy under similar FLOPs consumption since the FLOPs metric is more often adopted in the compact model research. To that effect, we train our supernet PSS-Net_M and PSS-Net_F using MobileNetV1 and MobilenetV2 as backbones respectively, and then extract the best subnets from PSS-Net_M and PSS-Net_F, whose FLOPs consumption is similar to the compact models for a fair comparison. Tab. 2 displays the performance comparison. As can be seen, our PSS-Net_M results in high-capacity subnets which not only surpass the com-

Method	Subnet Num.	Training	Storage
USNet	N	$< 4O_T$	$(1 + 0.02N)O_S$
MutualNet	N	$< 4O_T$	$(1 + 0.02N)O_S$
Pruning	N	NO_T	NO_S
PSS-Net	N	$< 3O_T$	$(1 + 0.02N)O_S$

Table 3: Complexity comparison of training and storage costs among existing resource-adaptive methods (Yu and Huang 2019b; Yang et al. 2020), channel pruning, and the proposed PSS-Net.

compact model methods significantly, but also are better than the original MobileNetV1/V2. Taking MobileNetV1 as an example, our PSS-Net_M provides a subnet that reduces the FLOPs of MobileNetV1 from 569M to 278M, and meanwhile increases the accuracy from 70.6% to 71.8%. Moreover, these compact methods produce static models for deployment while our PSS-Net_M offers switchable subnets to adapt the change of available resources, which greatly eases the model deployment in practical applications.

Complexity Comparison. We further compare the storage and training costs of our PSS-Net, resource-adaptive methods (Yu and Huang 2019b; Yang et al. 2020), and a compact method of channel pruning. Denote the training cost of the supernet as O_T and the storage cost as O_S . Given N subnets, we summarize the cost complexity in Tab. 3.

For resource-adaptive networks, k subnets of different sizes ($k = 4$ for USNet and MutualNet, $k = 3$ for PSS-Net) are trained in each batch, and thus the total training cost is not more than kO_T . The resource-adaptive network methods require to store BN parameters for each of the N subnets (the number of BN parameters for each MobileNetV1/V2 subnet is about 2% of the supernet’s parameters O_S), and thus the total storage overhead is about $(1 + 0.02N)O_S$. Most of the channel pruning methods require a complete training for each compact subnet in isolation, so the total training cost is about NO_T and the total storage cost is NO_S . Taking $N = 30$ as an example, PSS-Net achieves better performance than the channel pruning methods (Tab. 2) with about $\frac{1}{10}$ of the training cost and about $\frac{1}{20}$ of the storage cost compared to the channel pruning methods (Tab. 3).

Conclusion

In this paper, we have proposed Prioritized Subnet Sampling to train a resource-adaptive supernet, referred to as PSS-Net. Compared to existing resource-adaptive networks, our PSS-Net offers subnets with a better accuracy-resource trade-off by maintaining a set of subnet pools, each of which is conditioned on a particular resource constraint, and assigning priority to high-quality subnets for training. Consequently, our PSS-Net produces a set of high-quality subnets with different resource consumptions, thus allowing a fast switch of high-quality subnets for inference when the available resources vary. Besides, compared to the compact network methods such as pruning and NAS, our PSS-Net significantly reduces the training and storage cost. Extensive experiments on ImageNet using MobileNetV1/V2 as supernet have demonstrated the effectiveness of our approach.

References

- Bejnordi, B. E.; Blankevoort, T.; and Welling, M. 2020. Batch-shaping for learning conditional channel gated networks. In *Proceedings of the International Conference on Learning Representations (ICLR)*.
- Berman, M.; Pishchulin, L.; Xu, N.; Blaschko, M. B.; and Medioni, G. 2020. AOWS: Adaptive and optimal network width search with latency constraints. In *Proceedings of the IEEE/CVF Conference on Computer Vision and Pattern Recognition (CVPR)*, 11217–11226.
- Cai, H.; Gan, C.; Wang, T.; Zhang, Z.; and Han, S. 2020. Once-for-all: Train one network and specialize it for efficient deployment. In *Proceedings of the International Conference on Learning Representations (ICLR)*.
- Dai, X.; Zhang, P.; Wu, B.; Yin, H.; Sun, F.; Wang, Y.; Dukhan, M.; Hu, Y.; Wu, Y.; Jia, Y.; et al. 2019. Chamnet: Towards efficient network design through platform-aware model adaptation. In *Proceedings of the IEEE/CVF Conference on Computer Vision and Pattern Recognition (CVPR)*, 11398–11407.
- Deng, J.; Dong, W.; Socher, R.; Li, L.-J.; Li, K.; and Fei-Fei, L. 2009. Imagenet: A large-scale hierarchical image database. In *Proceedings of the IEEE/CVF Conference on Computer Vision and Pattern Recognition (CVPR)*, 248–255.
- Frankle, J.; and Carbin, M. 2018. The Lottery Ticket Hypothesis: Finding Sparse, Trainable Neural Networks. In *Proceedings of the International Conference on Learning Representations (ICLR)*.
- Gao, S.; Huang, F.; Pei, J.; and Huang, H. 2020. Discrete model compression with resource constraint for deep neural networks. In *Proceedings of the IEEE/CVF Conference on Computer Vision and Pattern Recognition (CVPR)*, 1899–1908.
- Guo, J.; Ouyang, W.; and Xu, D. 2020a. Channel pruning guided by classification loss and feature importance. In *Proceedings of the AAAI Conference on Artificial Intelligence (AAAI)*, 10885–10892.
- Guo, J.; Ouyang, W.; and Xu, D. 2020b. Multi-dimensional pruning: A unified framework for model compression. In *Proceedings of the IEEE/CVF Conference on Computer Vision and Pattern Recognition (CVPR)*, 1508–1517.
- Guo, S.; Wang, Y.; Li, Q.; and Yan, J. 2020a. Dmcp: Differentiable markov channel pruning for neural networks. In *Proceedings of the IEEE/CVF Conference on Computer Vision and Pattern Recognition (CVPR)*, 1539–1547.
- Guo, Z.; Zhang, X.; Mu, H.; Heng, W.; Liu, Z.; Wei, Y.; and Sun, J. 2020b. Single path one-shot neural architecture search with uniform sampling. In *Proceedings of the European Conference on Computer Vision (ECCV)*, 544–560.
- Han, S.; Pool, J.; Tran, J.; and Dally, W. 2015. Learning both Weights and Connections for Efficient Neural Network. In *Proceedings of the Advances in Neural Information Processing Systems (NeurIPS)*, 1135–1143.
- He, Y.; Lin, J.; Liu, Z.; Wang, H.; Li, L.-J.; and Han, S. 2018. Amc: Automl for model compression and acceleration on mobile devices. In *Proceedings of the European conference on computer vision (ECCV)*, 784–800.
- Howard, A. G.; Zhu, M.; Chen, B.; Kalenichenko, D.; Wang, W.; Weyand, T.; Andreetto, M.; and Adam, H. 2017. Mobilenets: Efficient convolutional neural networks for mobile vision applications. *arXiv preprint arXiv:1704.04861*.
- Huang, G.; Chen, D.; Li, T.; Wu, F.; van der Maaten, L.; and Weinberger, K. Q. 2018. Multi-scale dense networks for resource efficient image classification. In *Proceedings of the International Conference on Learning Representations (ICLR)*.
- Li, B.; Wu, B.; Su, J.; and Wang, G. 2020. Eagleeye: Fast sub-net evaluation for efficient neural network pruning. In *Proceedings of the European Conference on Computer Vision (ECCV)*, 639–654.
- Li, Y.; Lin, S.; Liu, J.; Ye, Q.; Wang, M.; Chao, F.; Yang, F.; Ma, J.; Tian, Q.; and Ji, R. 2021. Towards Compact CNNs via Collaborative Compression. In *Proceedings of the IEEE/CVF Conference on Computer Vision and Pattern Recognition (CVPR)*, 6438–6447.
- Lin, J.; Rao, Y.; Lu, J.; and Zhou, J. 2017. Runtime neural pruning. In *Proceedings of the Advances in Neural Information Processing Systems (NeurIPS)*, 2178–2188.
- Lin, M.; Ji, R.; Wang, Y.; Zhang, Y.; Zhang, B.; Tian, Y.; and Shao, L. 2020a. HRank: Filter Pruning using High-Rank Feature Map. In *Proceedings of the IEEE/CVF Conference on Computer Vision and Pattern Recognition (CVPR)*, 1529–1538.
- Lin, M.; Ji, R.; Zhang, Y.; Zhang, B.; Wu, Y.; and Tian, Y. 2020b. Channel pruning via automatic structure search. In *Proceedings of the International Joint Conference on Artificial Intelligence (IJCAI)*, 673 – 679.
- Liu, C.; Zoph, B.; Neumann, M.; Shlens, J.; Hua, W.; Li, L.-J.; Fei-Fei, L.; Yuille, A.; Huang, J.; and Murphy, K. 2018. Progressive neural architecture search. In *Proceedings of the European conference on computer vision (ECCV)*, 19–34.
- Liu, H.; Simonyan, K.; and Yang, Y. 2019. Darts: Differentiable architecture search. In *Proceedings of the International Conference on Learning Representations (ICLR)*.
- Liu, Z.; Mu, H.; Zhang, X.; Guo, Z.; Yang, X.; Cheng, K.-T.; and Sun, J. 2019. Metapruning: Meta learning for automatic neural network channel pruning. In *Proceedings of the IEEE/CVF International Conference on Computer Vision (ICCV)*, 3296–3305.
- Liu, Z.; Zhang, X.; Shen, Z.; Li, Z.; Wei, Y.; Cheng, K.-T.; and Sun, J. 2020. Joint Multi-Dimension Pruning. *arXiv preprint arXiv:2005.08931*.
- Lou, W.; Xun, L.; Sabet, A.; Bi, J.; Hare, J.; and Merrett, G. V. 2021. Dynamic-OFA: Runtime DNN Architecture Switching for Performance Scaling on Heterogeneous Embedded Platforms. In *Proceedings of the IEEE/CVF Conference on Computer Vision and Pattern Recognition (CVPR)*, 3110–3118.
- Ruan, X.; Liu, Y.; Li, B.; Yuan, C.; and Hu, W. 2021. DPFPS: Dynamic and Progressive Filter Pruning for Compressing Convolutional Neural Networks from Scratch. In

Proceedings of the AAAI Conference on Artificial Intelligence (AAAI), 2495–2503.

Sahni, M.; Varshini, S.; Khare, A.; and Tumanov, A. 2021. CompOFA: Compound Once-For-All Networks for Faster Multi-Platform Deployment. In *Proceedings of the International Conference on Learning Representations (ICLR)*.

Sandler, M.; Howard, A.; Zhu, M.; Zhmoginov, A.; and Chen, L.-C. 2018. Mobilenetv2: Inverted residuals and linear bottlenecks. In *Proceedings of the IEEE/CVF Conference on Computer Vision and Pattern Recognition (CVPR)*, 4510–4520.

Wang, D.; Li, M.; Gong, C.; and Chandra, V. 2021. Attentionas: Improving neural architecture search via attentive sampling. In *Proceedings of the IEEE/CVF Conference on Computer Vision and Pattern Recognition (CVPR)*, 6418–6427.

Wang, X.; Yu, F.; Dou, Z.-Y.; Darrell, T.; and Gonzalez, J. E. 2018. Skipnet: Learning dynamic routing in convolutional networks. In *Proceedings of the European Conference on Computer Vision (ECCV)*, 409–424.

Wang, Y.; Zhang, X.; Xie, L.; Zhou, J.; Su, H.; Zhang, B.; and Hu, X. 2020. Pruning from scratch. In *Proceedings of the AAAI Conference on Artificial Intelligence (AAAI)*, 12273–12280.

Yang, T.; Zhu, S.; Chen, C.; Yan, S.; Zhang, M.; and Willis, A. 2020. Mutualnet: Adaptive convnet via mutual learning from network width and resolution. In *Proceedings of the European Conference on Computer Vision (ECCV)*, 299–315.

Yang, T.-J.; Howard, A.; Chen, B.; Zhang, X.; Go, A.; Sandler, M.; Sze, V.; and Adam, H. 2018. Netadapt: Platform-aware neural network adaptation for mobile applications. In *Proceedings of the European Conference on Computer Vision (ECCV)*, 285–300.

Yu, J.; and Huang, T. 2019a. Autoslim: Towards one-shot architecture search for channel numbers. *arXiv preprint arXiv:1903.11728*.

Yu, J.; and Huang, T. S. 2019b. Universally slimmable networks and improved training techniques. In *Proceedings of the IEEE/CVF International Conference on Computer Vision (ICCV)*, 1803–1811.

Yu, J.; Jin, P.; Liu, H.; Bender, G.; Kindermans, P.-J.; Tan, M.; Huang, T.; Song, X.; Pang, R.; and Le, Q. 2020. Bignas: Scaling up neural architecture search with big single-stage models. In *Proceedings of the European Conference on Computer Vision (ECCV)*, 702–717.

Yu, J.; Yang, L.; Xu, N.; Yang, J.; and Huang, T. 2019. Slimmable neural networks. In *Proceedings of the International Conference on Learning Representations (ICLR)*.

Zoph, B.; and Le, Q. V. 2017. Neural architecture search with reinforcement learning. In *Proceedings of the International Conference on Learning Representations (ICLR)*.

Zoph, B.; Vasudevan, V.; Shlens, J.; and Le, Q. V. 2018. Learning transferable architectures for scalable image recognition. In *Proceedings of the IEEE/CVF Conference on Computer Vision and Pattern Recognition (CVPR)*, 8697–8710.

Slimmable Training

In Alg. 3, we elaborate slimmable training from USNet (Yu and Huang 2019b).

Algorithm 3: slimmable_training

Input: Supernet weight \mathbf{W} , list for subnet structure $subnet_list = \{\phi^{max}, \phi^t, \phi^{min}\}$.

Output: Supernet weight \mathbf{W} .

- 1: Get current data batch (x, y) ;
 - 2: $\phi^{max} = subnet_list[1]$;
 - 3: Forward the maximum subnet as $\hat{y} = \mathcal{N}_{\phi^{max}, \mathbf{w}}(x)$;
 - 4: Obtain the cross-entropy loss as $loss = CE(\hat{y}, y)$;
 - 5: Backward and accumulate loss as $loss.backward()$;
 - 6: Detach the gradient of \hat{y} as $\hat{y} = \hat{y}.detach()$;
 - 7: **for** ϕ^t in $subnet_list[2 :]$ **do**
 - 8: Forward subnet $y' = \mathcal{N}_{\phi^t, \mathbf{w}}(x)$;
 - 9: Conduct knowledge distillation between $\mathcal{N}_{\phi^{max}, \mathbf{w}}$ and $\mathcal{N}_{\phi^t, \mathbf{w}}$ Compute KL loss using Kullback-Leibler loss as $loss = KL(y', \hat{y})$;
 - 10: Backward and accumulate loss as $loss.backward()$;
 - 11: **end for**
 - 12: Update supernet weight \mathbf{W} as $optimizer.step()$;
 - 13: **Return** \mathbf{W} .
-

Training Settings

We use PyTorch as our training framework. The initial learning rate is set to 0.3 which is then adjusted by cosine annealing. SGD optimizer is adopted with a weight decay of 1e-4. We train our PSS-Net for a total of 250 epochs with a batch size of 1024.

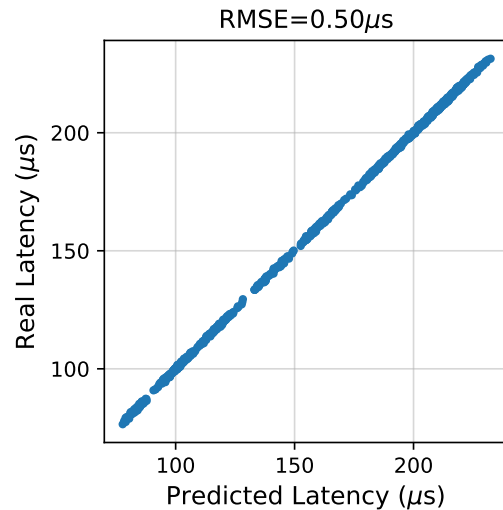


Figure 4: Predicted latency v.s. real latency. We sample 1,000 subnet structures using MobileNetV1 as the supernet. As can be seen, we obtain a very small RMSE of $0.5\mu s$ (root mean square error) between real latency and predicted latency, indicating an accurate prediction of our lookup tables.

Backbone	Lower Bound	Method	FLOPs (M)	Acc (%)
MBV1	0.25	MutualNet	13	45.5
			569	72.4
		PSS-Net	13	50.8 (+5.3)
			569	72.8 (+0.4)
MBV2	0.7	MutualNet	57	64.2
			301	72.9
		PSS-Net	57	65.4 (+1.2)
	301		73.1 (+0.2)	
	0.8	MutualNet	73	66.0
			301	73.2
PSS-Net		73	66.8 (+0.8)	
		PSS-Net	301	73.5 (+0.3)

Table 4: Performance comparison with MutualNet (Yang et al. 2020) under different low bounds of subnets.

Latency Lookup Table

We respectively test the CPU latency and GPU latency on a single core of *Intel Xeon Platinum 8268* CPU and on a single *NVIDIA Tesla V100* GPU. To realize a quick calculation of resource consumption $\mathcal{C}(\cdot)$, we construct lookup tables of CPU and GPU latencies for during our PSS-Net training. To this end, the most naive approach is to pre-compute the practical consumption on the target platform for all subnet structures $\phi^t \in \mathcal{S}$. However, the large volume of \mathcal{S} makes it intractable. Instead, we choose to compute the latency of each subnet block in \mathcal{S} and build latency tables for these blocks. During PSS-Net training, the latency of a given subnet structure is predicted by summing up the latencies of the blocks making up this subnet. In Fig. 4, we randomly sample 1,000 subnet structures using MobileNetV1 as the supernet, and show the actual GPU latencies of these subnets v.s. their block summation from the lookup tables. As can be seen from Fig. 4, the predicted latency is very close to the real latency, which indicates that our lookup tables are very accurate and reliable.

Ablation Studies

We further conduct ablation studies to analyze the effectiveness of our PSS-Net. All the experiments are conducted using MobileNetV1 as the supernet which is trained under the FLOPs constraint.

Low Bound of Subnets

Recall that we set o_i^{max} to be the same as the channel number of the i -th layer in the backbone network, and the low bound of subnets $o_i^{min} = 0.75 \cdot o_i^{max}$. In this subsection, we consider different low bounds adopted by MutualNet (Yang et al. 2020) and show the experimental results in Tab. 4. As can be seen, our PSS-Net shows consistently better performance than MutualNet when the low bounds are set to different scales, which well demonstrates the effectiveness of our PSS-Net.

Pool	Acc (%)			
	k=1	k=5	k=10	k=20
300M	71.4	72.3 (+0.9)	72.3 (+0.9)	72.4 (+1.0)
400M	72.7	72.9 (+0.2)	72.9 (+0.2)	72.9 (+0.2)
500M	73.7	73.8 (+0.1)	73.8 (+0.1)	73.8 (+0.1)
Avg. Boost	/	+0.4	+0.4	+0.43

Table 5: BN calibration for subnets within top- k performance metrics.

Subnet	FLOPs	Acc _{PSS} (%)	Acc _{Fine-tune} (%)
A	300M	72.3	71.9 (-0.4)
B	400M	73.0	72.7 (-0.3)
C	500M	73.8	73.5 (-0.3)

Table 6: Performance comparison before/after fine-tuning the best subnets.

BN Calibration.

Our PSS-Net follows the slimmable training paradigm which requires BN calibration for each subnet. However, the large volume of subnet space disables one-by-one calibration. Luckily, our introduced subnet pool encourages to collect more high-quality subnets. Consequently, we only need to calibrate k subnets within top- k performance metrics, and then pick the one with the best accuracy. To verify this, in Tab. 5, we choose different values of k and show the best subnets after BN calibration, which are constrained by the FLOPs of 300M, 400M and 500M. When $k \geq 2$, better subnets can be observed than simply considering the top-1. However, the performance gains are limited when $k > 5$, which indicates the best subnets fall into these subnets within top-5 performance metrics. Thus, we only need to pick up 5 subnets in each pool for BN calibration, which is also our setting in all the experiments.

Subnet Fine-tuning.

As mentioned in the introduction section, existing researches suffer the problem of subnet mismatch, which causes insufficient training of high-quality subnets. Our PSS-Net solves this problem by giving priority to sampling high-quality subnets in the subnet pool. In this subsection, we further investigate whether the best subnets have been well trained in PSS-Net. To this end, we select the best subnets from the 300M-, 400M-, and 500M-subnet pools, and further fine-tune these subnets for 25 epochs. Tab. 6 shows the performance comparison before/after fine-tuning. As can be seen, fine-tuning incurs slight performance drops in all the three cases. This experiment demonstrates that our high-quality subnets are already well trained and our PSS-Net well solves the subnet mismatch problems.